Geoelectrical measurement and modeling of biogeochemical breakthrough behavior during microbial activity

Lee Slater[1*], Fred Day-Lewis[2], Dimitrios Ntarlagiannis[1], Michael O'Brien[1] and Nathan Yee[3]

[1]Dept. of Earth & Environmental Sciences, Rutgers University, Newark, NJ

[2]USGS, Office of Groundwater, Branch of Geophysics, Storrs CT

[3]School of Environmental Sciences, Rutgers University, New Brunswick, NJ

** corresponding author*

Final copy as submitted to Geophysical Research Letters for publication as: Slater, L., Day-Lewis, F.D., Ntarlagiannis, D., O'Brien, M., and Yee, N., 2009, Geoelectrical measurement and modeling of biogeochemical breakthrough behavior during microbial activity: Geophysical Research Letters, v. 36, L14402, doi:10.1029/2009GL038695.

ABSTRACT

We recorded bulk electrical conductivity (σ_b) along a soil column during microbially-mediated selenite oxyanion reduction. Effluent fluid electrical conductivity and early time σ_b were modeled according to classic advective-dispersive transport of the nutrient medium. However, σ_b along the column exhibited strongly bimodal breakthrough which cannot be explained by changes in the electrical conductivity of the pore fluid. We model the anomalous breakthrough by adding a conduction path in parallel with the fluid phase, with a time dependence described by a microbial population-dynamics model. We incorporate a delay time to show that breakthrough curves along the column satisfy the same growth model parameters and offer a possible explanation based on biomass-limited growth that is delayed with distance from influent of the nutrient medium. Although the mechanism causing conductivity enhancement in the presence of biomass is uncertain, our results strongly suggest that biogeochemical breakthrough curves have been captured in geoelectrical datasets.

INTRODUCTION

Biogeophysics is an emerging geoscience discipline that explores the links between subsurface microbial processes, microbial alterations to geologic materials, and geophysical signatures. An expanding volume of literature demonstrates that electrical signals result from the geochemical and physical alteration of porous media associated with microbe-mineral transformations of electrically conductive mineral phases. The geoelectrical signatures arising during biomineralization of metallic iron sulfide (FeS) by sulfate-reducing microorganisms have received almost exclusive attention [*Slater et al.*, 2007; *Williams et al.*, 2005]. The electrical properties of FeS minerals clearly support geoelectrical monitoring of FeS biomineralization, e.g. the mean electrical conductivity of pyrite is estimated to be 5.6×10^3 S/m [*Abraitis et al.*, 2004]. The enhancement in electrochemical polarization of the mineral-fluid interface, combined with increases in bulk conductivity (σ_b)following extensive biomineralization, have confirmed that geoelectrical monitoring is a viable approach for tracking the progress of remedial treatment efforts to stimulate microbial mineralization of electrically conductive heavy metals *in situ* [*Slater et al.*, 2007; *Williams et al.*, 2005].

Although microbial processes demonstrably result in the precipitation of semi-metallic or non-metallic minerals, the sensitivity of geoelectrical methods to such processes is unreported. An obvious example is microbial calcite precipitation [*Fortin et al.*, 1997], e.g. bacterial hydrolysis of urea [*Fujita et al.*, 2000]. Here, we report on measurements of σ_b made during microbially-mediated reduction of selenite [Se^{4+}, SeO_3^{2-}] and resulting precipitation of elemental selenium [Se^0]. Se^0 is classified as a semi-metallic mineral, being a relatively poor conductor (e.g. *Emsley* [1998] reports ~100 S/m). We chose to work with Se^0 because precipitation of this bright red mineral provides visible evidence of microbial activity and it is a known contaminant at high concentration.

We observe compelling increases in σ_b resulting from the microbially-mediated precipitation of Se^0. We demonstrate that this response can be modeled using an electrical model based on time-dependant electrolytic and microbe-related conductivity terms in parallel. We couple the commonly applied Archie model with a 1D model of advective-dispersive solute transport to simulate the experimental increases in σ_b resulting from transport of the nutrient medium and associated changes in pore-fluid conductivity. Delayed increases in σ_b are observed

after breakthrough of the nutrient medium at the outflow, explainable only by evolution of an additional conductive phase that we attribute to growth of the selenite reducers. We represent this additional, time-varying conductivity using a commonly applied model of microbial growth. This fact, coupled with the delayed onset of this biogeophysical signature with distance from the influent (source of nutrient media) strongly indicates that microbial growth has an observable geoelectrical signature.

METHODS

Soil samples were retrieved from Belews Lake (North Carolina, USA), a site contaminated by selenium-laden wastewater from a coal-burning power plant [*Lemly*, 1997], and screened for the presence of selenium-reducing bacteria by establishing enrichment cultures in a minimal salts medium composed of K_2HPO_4 (0.225 g/L), KH_2PO_4 (0.225 g/L), NaCl (0.460 g/L), $(NH_4)_2SO_4$ (0.225 g/L), $MgSO_4 \cdot 7H_2O$ (0.117 g/L), $NaHCO_3$ (0.05 g/L), $FeCl_3$ (0.005 g/L), yeast extract (0.5 g/L), casamino acids (0.1 g/L), lactate (1.0 g/L), and trace element solution (1 mL/L). The nutrient medium contained higher nutrient concentrations than the minimal salts medium and was supplemented with 1mM of either selenite (SeO_3^{2-}) or selenate (SeO_4^{2-}) and incubated in a shaker at 150 rpm at 30^{o}C for over 72 hours. A reddening of the enrichment culture was observed, diagnostic of Se^0 precipitation resulting from microbially-mediated selenium oxyanion reduction. The enrichment culture was plated onto selenium-containing agar to isolate the Se-reducing microorganisms. After several serial dilutions, an isolate designated BL-2 and capable of reducing both selenate and selenite was obtained. Based on 16S rRNA sequencing, BL-2 was shown to be 99.9% related to *Enterobacter cloacae*, a known selenium reducer.

Soil samples were mixed (20% by weight) with Ottawa sand (99.8% quartz, 600-800 µm)and packed into two clear PVC columns (length = 30 cm; diameter = 5 cm). The first (active) column contained the active microbial community whereas a second (control) column (run after the active column) was packed with an autoclaved (15 minutes at 121^o C) soil. A continual flow of a minimal salts medium (excluding selenium) ($\sigma_{w(0)}$ = 0.19 S/m) was first established for three days at a volumetric discharge (Q) of 219 mL/day, equivalent to ~ 1 pore-volume/day based on a measured (by weight loss on drying) porosity of 0.38 ± 0.01) (Figure 1). Following stabilization of electrical conductivity (indicating saturation), the nutrient medium ($\sigma_{w(in)}$ = 0.29 S/m, containing 1mM (21 mg/L) sodium selenite) was introduced into both columns (defining Day 0). An average Q of 219 mL/day was maintained for the active column, except for a 4-hr period on Day 3, when the pump was shut off to fix an electrode problem. The active and control experiments were terminated on Days 17 and 10, respectively. The experiment was run at a temperature of 22 +/- 2 ^{o}C.

Fluid conductivity (σ_w) and pH of inflow and outflow were recorded using benchtop probes (twice daily). Influent and effluent samples on the active column were collected daily and analyzed for total dissolved selenium using Inductively Coupled Plasma Mass Spectroscopy (ICP-MS). Intensity of peaks at four different wavelengths for selenite were measured and referenced to known standards. Bulk electrical conductivity was determined from electrical potentials (ΔV) measured using six Ag-AgCl point electrodes at 3-cm spacing along the column (Figure 1). All measurements were made using a multi-channel resistivity meter (100 MOhm input impedance) with the injection of 1 s current (I) waveform between Ag-AgCl coil electrodes (C1 and C2) at the column ends. Measurements of ΔV were collected simultaneously on five channels (E1-E2, E2-E3 E3-E4, E4-E5 and E5-E6, with center points from 9-21 cm from the

influent) between 3-7 times per day, with higher sampling rates during early breakthrough. The σ_b of the soil volume between each electrode pair was calculated as $\sigma_b = (I/\Delta V)(l/A)$, where l is the inter-electrode distance and A is the column's cross-sectional area (19.6 cm^2). This provided σ_b estimates for five 59-cm^3 sections of soil.

RESULTS

Aqueous geochemistry and visible observations

Total dissolved selenium concentrations in the effluent samples in the active column decreased from approximately 18 mg/L on Day 0 to approximately 14 mg/L on Day 17 with concentration decreasing at a progressively greater rate with time (data not shown for brevity). Decreases in dissolved selenium concentration at the effluent are consistent with microbial selenite reduction and precipitation of Se^0. Visible evidence for the accumulation of Se^0 was first apparent in the active column at Day 9 with extensive precipitation by Day 17 (Figure 1). No visible precipitate was observed in the control column. Effluent pH of active and control columns showed no variation outside of the range of 7.0-7.5 for which the influent was balanced. Transition to the nutrient medium (on Day 0) resulted in a 53% increase in outflow conductivity ($\sigma_{w(of)}$) of the active column from 0.19 S/m to 0.30 S/m by Day 5 (errors are ~3.2%) (Figure 2a, symbols). The influent conductivity varied by only ~2% during this time. Given the ~1 pore volume/day flow rate, ~5 pore volumes were required to reach equilibrium with the new influent. After Day 5 $\sigma_{w(of)}$ varied between 0.290-0.302 S/m.

Bulk electrical conductivity

The temporal response of measured σ_b in the active column (Figure 2b,c, symbols) is characterized by two increases (that then plateau), most obvious in the responses at 12 cm and 15 cm. The first increase in σ_b occurs between 0-3 days at all column locations as a result of fluid displacement by the more electrically conductive nutrient medium. The observed increase in σ_b is ~50% at 9 cm, 12 cm and 18 cm along the column, whereas the increase is ~35% at 15 cm and 21 cm. A similar response to nutrient breakthrough was observed in the control column with maximum ~30% σ_b increases observed.

The onset of the late-time increase in σ_b (as visibly estimated from the inflection point) in the active column is delayed increasingly with distance from the influent. Closest to the influent (E1-E2) the late-time increase partially overlaps the response associated with the nutrient medium, whereas at the far end of the column, the second increase is very delayed, occurring at ~12 days (E4-E5 and E5-E6). Although the inflection point is delayed at 12 cm by ~4 days relative to at 9 cm, the increases plateau at approximately the same σ_b (representing an additional ~ 50% increase above that caused by the selenite medium). The inflection point at 15 cm occurs at about 10 days and results in an additional ~20% increase in σ_b. The inflection points at 18 cm and 21 cm are not well defined but occur at ~ 13 days and result in only an additional ~10% increase in σ_b. In general, the timing of the inflection point increases, whereas the magnitude of change in σ_b decreases, with distance from the influent. However, the late-time increases in σ_b exhibit a similar shape throughout the column. The control column showed no late-time increase in σ_b with changes less than 5% after the nutrient breakthrough.

MODELING

Solute breakthrough

We first modeled $\sigma_{w(of)}$ and σ_b along the column by combining (1) a 1D analytical model [*Ogata and Banks*, 1961] for advective-dispersive solute transport with a continuous source, and (2) an Archie expression for the electrolytic conductivity (σ_{el}): $\sigma_b = \sigma_{el} = F^{-1}\sigma_w = \sigma_w \phi^m$, where σ_w is the conductivity of the pore fluid (determined from the solute transport model), F is the electrical formation factor, ϕ is the porosity, and m is the Archie cementation factor. We neglect surface conduction because of the high σ_w of the nutrient medium. The parameters of this coupled model are specific discharge (q), fluid conductivity before injection ($\sigma_{w(0)}$), input fluid conductivity ($\sigma_{w(in)}$), dispersivity (α), ϕ and m. With the exception of α, all parameters are constrained by data. Values for $\sigma_{w(0)}$, $\sigma_{w(in)}$, q and ϕ (assumed constant for simplicity) were given in the methods description. In the interest of model simplicity, we have not incorporated the 4-hr shutdown of the pump on Day 3 but instead assume q = 0.108 m/day as measured on Days 0, 3 (after turning on the pump) and 6. A representative value for m was derived by first estimating F by least-squares regression of σ_b versus $\sigma_{w(of)}$ (control column) for the two locations closest to the outflow, where we approximate the conductivity of the pore fluid (σ_w) as $\sigma_{w(of)}$. This gave an estimate of $F = 8 \pm 0.1$ ($R^2 = 0.76$), yielding $m \approx 2.1$ for $\phi = 0.38$. Figure 2a (solid line) shows the fit of the model to $\sigma_{w(of)}$, whereas Figure 2b,c (solid lines) shows the fit to σ_b. We cannot fit $\sigma_{w(of)}$ for Day 3 but attribute this to the shutdown of the pump. The early rise (solute-controlled) σ_b data at all locations can be adequately fit if m is varied between 2.0 and 2.15 (with fixed ϕ and D). A limited variation in m is reasonable given minor differences in soil packing. Manual calibration of the transport model against measured σ_b and $\sigma_{w(of)}$ yielded an estimate of α=0.17 m. Although simulated $\sigma_{w(of)}$ and σ_b do not perfectly match the experimental data, our model results conclusively demonstrate that advective-dispersive transport cannot explain the late-time increases in σ_b. Indeed, the late-time changes in σ_b cannot be attributed to changes in the fluid phase, as $\sigma_{w(of)}$ does not show bimodal breakthrough (Figure 2a, symbols). Although sorption could conceivably impact σ_b, we consider it unlikely as (1) it was not needed to model $\sigma_{w(of)}$ breakthrough in the active column, and (2) bimodal breakthrough curves were not observed in the control column.

Biogeochemical breakthrough

We contend that increases in σ_b must represent a biogeochemical transformation associated with microbial growth. The complexity of this process prevents any effort to model this σ_b increase in terms of reaction products (e.g. precipitation of selenium), nor do we have sufficient data to constrain such a model. However, microbial population dynamics are commonly represented by growth models that predict an early exponential increase, followed by diminishing growth, and finally an asymptotic approach to equilibrium, where the rates of production and death are equal. It is thus reasonable to assume that, if σ_b is a response to the microbially-mediated selenite reduction, then the shape of the σ_b curves might exhibit the sigmoidal shape of such growth curves. Indeed, the late-time σ_b response shows all the characteristics of a typical population growth curve, only observed in the microbially-active column.

In order to test our hypothesis, we add a conduction term (σ_{mg}) associated with microbial growth in parallel to σ_{el}, to generate the model, $\sigma_b = \sigma_{el} + \sigma_{mg} = \sigma_w \phi^m + \sigma_{mg}$. This formulation implicitly assumes that the two conduction pathways act in parallel. Verification of this assumption would require information for the geometry of the evolving conductive phase, which is beyond the scope of this study. There are a wide number of growth models with similar shapes (e.g. Verhulst's logistic equation and modifications thereof) that might reproduce the time evolution of σ_s. We use the Gompertz curve [*Windsor*, 1932], which has only three parameters and does not require specification of an initial 'population', in our case the unknown reaction products that contribute to σ_{mg}. Using the Gompertz curve we define $\sigma_{mg} = a \exp[b \exp(ct)]$ where *a* is the late-time population, *b* controls the curve temporally, and *c* controls the approach to equilibrium. The fit of the σ_b data to this coupled solute-electrical-microbial growth model is shown in Figure 2c. The fits were generated using spatially uniform parameters *b*=-5 and *c*=-0.7 day^{-1} (*a* was a fitting parameter varying between 0.002-0.012 S/m) and invoking a delay time for initiation of growth that increases along the column from 6 to 18 times the advective arrival time. Although we could have fit the data by varying *b* along the column and using a constant delay time, we believe that an increasing delay is more consistent with the selenite reduction process, as we discuss below. Furthermore, this approach illustrates that the shape of the σ_b response (defined by *b* and *c*) is preserved along the column; i.e. the same biogeochemical process is observed throughout, only the onset of the process is delayed increasingly with distance from the influent, and the maximum population decreases away from the nutrient source.

DISCUSSION

We have shown that the observed σ_b response is consistent with advective-dispersive transport of the nutrient medium, coupled with an increase in σ_b exhibiting the sigmoidal shape of curves commonly used to model cell growth. We propose a basic conceptual framework for the biogeochemical transformations occurring in this column, defined by three stages registered in the σ_b response: (1) a lag phase during which microbial growth is occurring at a rate insufficient to generate significant (i.e. electrically detectable) growth products (defined to include the biomass); (2) a period of increasing growth rates, accompanied by rapid accumulation of growth products; and (3) a final stage of declining growth rates that limit the accumulation of growth products to some maximum value. The observed increase in delay time with distance along the column is consistent with this conceptual framework as the supply of nutrients at a given point is limited by consumption closer to the influent.

The question to consider is, "Why does the accumulation of growth products associated with the microbial growth generate an electrical signature?" The simplest explanation is that progressive precipitation of elemental selenium forms a new conduction path in parallel with σ_{el}. Given selenium's conductivity (~100 S/m [*Emsley*, 1998]), this is plausible. Mass balance analysis of selenite from ICPMS measurements indicates that Se^0 filled ~0.6 % of the pore space (~0.2% total volume). A simple mixing model [*Keller*, 1987, Eq. 46] based on a uniform medium (of 0.04 S/m) with 0.2% spherical inclusions of 100 S/m, yields a σ_b of 0.18 S/m, greater than the change observed here. However, visual observations of Se precipitation (Figure 1) do not correlate with the σ_b response. Given that the σ_b curves are delayed along the column, and exhibit greatest changes at 9 and 12 cm, we would expect the Se^0 precipitation to be most

visible extensive at these locations. Instead, Se^0 was first observed as a patchy precipitation along the column and did not develop in any obvious order with time.

We tentatively offer an alternative explanation whereby the growth in the biomass of the Se^{4+} reducers is responsible for the σ_b response. Biomass growth would be expected to first occur closer to the influent source of the nutrient medium, and be delayed away from the source i.e. towards the effluent. Initially, the accumulation of biomass increases the rate of growth (as supported by decreasing dissolved selenium concentrations at the outflow with time) assuming that the growth rate is limited by the bacteria concentration. The microbial concentration subsequently begins to limit growth until a critical concentration when the system reaches steady state. From the σ_b curves the critical mass fraction would be inferred to have been reached at approximately 7 days at 9 cm and 14 days at 12 cm. In this conceptual model, whenever any σ_b curve reached steady state it indicates that, upstream (i.e. toward influent) of that point, the biomass went to the critical concentration being characteristic of steady state. Presumably this critical concentration was not reached at points further from the influent before the experiment was terminated. Other explanations for the subdued response towards the effluent could possibly include chemotactic movement of cells towards influent, and/or spatial variability in the population distribution not described by this simple growth model.

This latter explanation requires that the biomass is an electrical conductor, partly supported by recent work indicating that biomass growth and biofilm development increase the interfacial conductivity of soils [*Aal et al.*, 2004; *Davis et al.*, 2006]. Electrically conductive biofilms have been postulated in order to model self-potential anomalies over contaminated sites [*Naudet and Revil*, 2005]. However, proving that the electrical conductivity of biomass is sufficient to drive the observed response requires further investigation.

CONCLUSIONS

We have demonstrated an electrical conductivity response during microbial activity exhibiting the characteristics of models often used to describe microbial processes. Although experimental effluent fluid electrical conductivity was consistent with classic advective-dispersive transport, bulk electrical conductivity along the column exhibited bimodal breakthrough that cannot be explained by changes in the fluid phase. We demonstrated that evolution of a new conduction term in parallel with the electrolytic conductivity and with the time dependence of a classical microbial population dynamics model could explain the anomalous bulk conductivity breakthrough. In the same way that electrical measurements have been used to investigate solute transport, our work suggests that electrical measurements could also be used to infer biogeochemical transformations at spatiotemporal scales impossible to examine using conventional measurements. We suggest that our results provide the first evidence of biogeochemical breakthrough curves in geoelectrical data. Our work points to the potential of electrical methods to non-invasively monitor biogeochemical transformations associated with microbial activity and thus provide insight into natural attenuation of contaminants and the efficacy of engineered remediation. Further work is needed to elucidate the mechanisms causing conductivity enhancement during microbial growth.

ACKNOWLEDGEMENTS

This material is based upon work supported by the National Science Foundation under grant EAR-0433729, with additional support from the U.S.G.S. Toxic Substances Hydrology

Program. We thank Chi Zhang (Rutgers-Newark) for valuable assistance in laboratory work. We thank Sue Brantley (Pennsylvania State University) for enlightening discussions at the AGU Chapman Conference on Biogeophysics, Portland, ME, Oct 13-16, 2008. We also thank Burke Minsley and Rory Henderson for constructive comments that improved this manuscript.

REFERENCES

Aal, G. Z. A., E. A. Atekwana, and L. D. Slater (2004), Effects of microbial processes on electrolytic and interfacial electrical properties of unconsolidated sediments, *Geophysical Research Letters*, *31*(12).

Abraitis, P. K., R. A. D. Pattrick, and D. J. Vaughan (2004), Variations in the compositional, textural and electrical properties of natural pyrite: a review, *International Journal of Mineral Processing*, *74*(1-4), 41-59.

Davis, C. A., E. Atekwana, E. Atekwana, L. D. Slater, S. Rossbach, and M. R. Mormile (2006), Microbial growth and biofilm formation in geologic media is detected with complex conductivity measurements, *Geophysical Research Letters*, *33*, L18403, doi:18410.11029/12006GL027312.

Emsley, J. (1998), The Elements., 3rd ed., Clarendon Press, New York.

Fortin, D., F. G. Ferris, and T. J. Beveridge (1997), Surface-mediated mineral development by bacteria, Mineralogical Soc America.

Fujita, Y., E. G. Ferris, R. D. Lawson, F. S. Colwell, and R. W. Smith (2000), Calcium carbonate precipitation by ureolytic subsurface bacteria, Geomicrobiol. J., 17(4), 305-318.

Lemly, A. D. (1997), Ecosystem recovery following selenium contamination in a freshwater reservoir, *Ecotox. Environ. Safe.*, *36*(3), 275-281.

Naudet, V., and A. Revil (2005), A sandbox experiment to investigate bacteria-mediated redox processes on self-potential signals, *Geophysical Research Letters*, *32*(11), 4.

Ogata, A., and R. B. Banks (1961), A solution of the differential equation of longitudinal dispersion in porous media, U.S. Geological Survey, Professional Paper No. 411-A.

Slater, L., D. Ntarlagiannis, Y. Personna, and S. S. Hubbard (2007), Pore-scale Spectral Induced Polarization (SIP) signatures associated with FeS biomineral transformations, *Geophysical Research Letters*, *34*, L21404, doi 21410.21029/22007GL031840.

Williams, K. H., D. Ntarlagiannis, L. Slater, A. Dohnalkova, S. S. Hubbard, and J. F. Banfield (2005), Geophysical imaging of stimulated microbial biomineralization, *Environmental Science & Technology*, *39*, 7592-7600.

Windsor, P. (1932), The Gompertz curve as a growth curve, *Proceedings of the National Academy of Sciences*, *18*(1), 1-8.

Figures

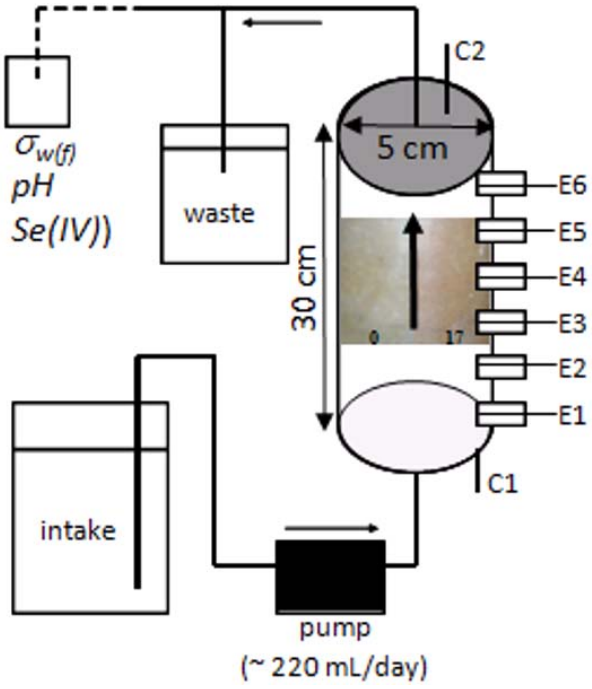

Figure 1. Figure 1. Schematic of experiment setup showing flow-through configuration, measurement electrode locations (E1-E6) spaced 3 cm apart, and current injection electrodes. Image insets in the column body show characteristic color changes between E3-E4, between days 0 (left) and 17 (right), due to microbially-induced Se precipitation.

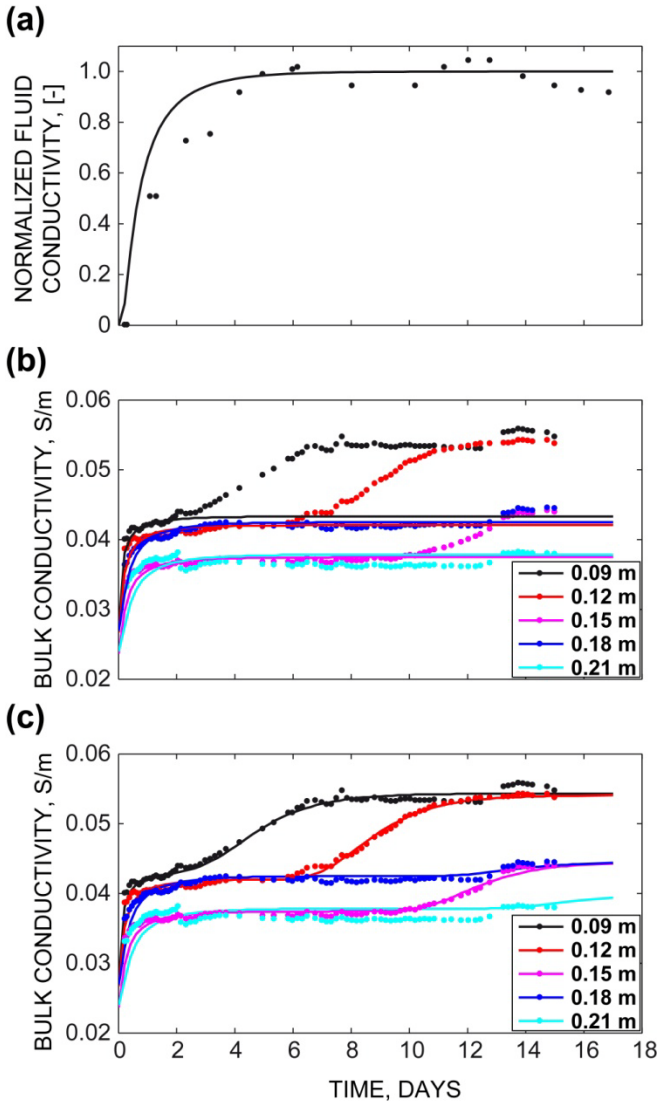

Figure 2. Figure 2. Active column results (a) Observed (symbols) and modeled (line) outflow fluid conductivity ($\sigma_{w(of)}$) normalized by inlet ($\sigma_{w(in)}$) and initial ($\sigma_{w(0)}$) fluid conductivities as ($\sigma_{w(of)}$ - $\sigma_{w(0)}$)/($\sigma_{w(in)}$- $\sigma_{w(0)}$); (b) observed (symbols) and modeled (lines) bulk conductivity (σ_b) assuming advective-dispersive transport and electrolytic conduction; and (c) observed (symbols) and modeled (lines) σ_b for advective-dispersive transport with electrolytic conduction and microbially-induced conduction according to the Gompertz growth model.